Fraunhofer Institut Techno- und Wirtschaftsmathematik

R. Ciegis, O. Iliev, S. Rief, K. Steiner

On Modelling and Simulation of Different Regimes for Liquid Polymer Moulding

Berichte des Fraunhofer ITWM, Nr. 63 (2004)

© Fraunhofer-Institut für Techno- und Wirtschaftsmathematik ITWM 2004

ISSN 1434-9973

Bericht 63 (2004)

Alle Rechte vorbehalten. Ohne ausdrückliche, schriftliche Genehmigung des Herausgebers ist es nicht gestattet, das Buch oder Teile daraus in irgendeiner Form durch Fotokopie, Mikrofilm oder andere Verfahren zu reproduzieren oder in eine für Maschinen, insbesondere Datenverarbeitungsanlagen, verwendbare Sprache zu übertragen. Dasselbe gilt für das Recht der öffentlichen Wiedergabe.

Warennamen werden ohne Gewährleistung der freien Verwendbarkeit benutzt.

Die Veröffentlichungen in der Berichtsreihe des Fraunhofer ITWM können bezogen werden über:

Fraunhofer-Institut für Techno- und
Wirtschaftsmathematik ITWM
Gottlieb-Daimler-Straße, Geb. 49

67663 Kaiserslautern
Germany

Telefon: +49 (0) 6 31/2 05-32 42
Telefax: +49 (0) 6 31/2 05-41 39
E-Mail: info@itwm.fraunhofer.de
Internet: www.itwm.fraunhofer.de

Vorwort

Das Tätigkeitsfeld des Fraunhofer Instituts für Techno- und Wirtschaftsmathematik ITWM umfasst anwendungsnahe Grundlagenforschung, angewandte Forschung sowie Beratung und kundenspezifische Lösungen auf allen Gebieten, die für Techno- und Wirtschaftsmathematik bedeutsam sind.

In der Reihe »Berichte des Fraunhofer ITWM« soll die Arbeit des Instituts kontinuierlich einer interessierten Öffentlichkeit in Industrie, Wirtschaft und Wissenschaft vorgestellt werden. Durch die enge Verzahnung mit dem Fachbereich Mathematik der Universität Kaiserslautern sowie durch zahlreiche Kooperationen mit internationalen Institutionen und Hochschulen in den Bereichen Ausbildung und Forschung ist ein großes Potenzial für Forschungsberichte vorhanden. In die Berichtreihe sollen sowohl hervorragende Diplom- und Projektarbeiten und Dissertationen als auch Forschungsberichte der Institutsmitarbeiter und Institutsgäste zu aktuellen Fragen der Techno- und Wirtschaftsmathematik aufgenommen werden.

Darüberhinaus bietet die Reihe ein Forum für die Berichterstattung über die zahlreichen Kooperationsprojekte des Instituts mit Partnern aus Industrie und Wirtschaft.

Berichterstattung heißt hier Dokumentation darüber, wie aktuelle Ergebnisse aus mathematischer Forschungs- und Entwicklungsarbeit in industrielle Anwendungen und Softwareprodukte transferiert werden, und wie umgekehrt Probleme der Praxis neue interessante mathematische Fragestellungen generieren.

Prof. Dr. Dieter Prätzel-Wolters
Institutsleiter

Kaiserslautern, im Juni 2001

On Modelling and Simulation of different Regimes for Liquid Polymer Moulding

R. Čiegis, O. Iliev, S. Rief, K. Steiner

April 28, 2004

Abstract

In this paper we consider numerical algorithms for solving a system of nonlinear PDEs arising in modeling of liquid polymer injection. We investigate the particular case when a porous preform is located within the mould, so that the liquid polymer flows through a porous medium during the filling stage. The nonlinearity of the governing system of PDEs is due to the non-Newtonian behavior of the polymer, as well as due to the moving free boundary. The latter is related to the penetration front and a Stefan type problem is formulated to account for it. A finite-volume method is used to approximate the given differential problem. Results of numerical experiments are presented.

We also solve an inverse problem and present algorithms for the determination of the absolute preform permeability coefficient in the case when the velocity of the penetration front is known from measurements.

In both cases (direct and inverse problems) we emphasize on the specifics related to the non-Newtonian behavior of the polymer. For completeness, we discuss also the Newtonian case. Results of some experimental measurements are presented and discussed.

Keywords: *Liquid Polymer Moulding, Modelling, Simulation. Infiltration, Front Propagation, non-Newtonian flow in porous media*

1 Introduction

Composite materials are widely used in automotive, aerospace, railroad, marine and many other industries. Liquid composite moulding is a family of technologies to manufacture composite materials. These technologies (see, e.g., [5, 35, 38, 43]) are of strong economical interest for manufacturing high quality composite parts. The essence of the discussed technologies is that a dry fibrous mat, which forms a porous preform, is located within the mould, and after that the liquid polymer is injected. In this way an accurate orientation of the fibers within the composite parts is achieved, making moulding parts with desired mechanical properties. In order to reduce the production costs of manufactured parts, mathematical modeling and numerical simulation are more and more extensively used at the designing stage. Since the filling of the mould is the most critical part of the process, most of the effort is concentrated on its study. The review articles [9, 39] give an impression about most of the mathematical models and numerical algorithms developed in this area. The great part of the models (see, e.g., [9] and references therein) use the linear Darcy model to describe the liquid polymer flow through the porous preform, the latter being considered in rigid body approximation. It should be noted, that such models are not valid for the flow of non-Newtonian fluids. Moreover, they do not account for the compressibility of the fibrous mat and, therefore, these models have a limited range of applicability in modeling polymer moulding. More advanced models consider either the coupled problem for Newtonian fluids in deformable porous media (see, e.g., [1, 18, 19, 20, 21, 39]), or the flow of a non-Newtonian fluid in a rigid porous medium (see, e.g., [44]). The most complete formulation concerning non-Newtonian flow in deformable porous medium is still not well studied.

Several challenging mathematical problems have to be solved in connection with simulation of liquid polymer moulding. Among them are developing of accurate numerical algorithms for solving the nonlinear free boundary direct problems, analysing and solving inverse problems (e.g., parameter estimation, etc.). This paper concerns several aspects of the modeling of LPM processes. These are:

(i) presenting a complete model for flow of non-Newtonian fluids in deformable porous media;

(ii) solving an inverse problem for determining permeability in the case when the penetration front is known from the measurements;

(iii) developing a finite volume algorithm for solving the 1-D direct problem.

First of all, a complete model for flow of non-Newtonian fluids in deformable porous media is listed. Curing (i.e., polymerization) is also accounted for. The model assumes a sharp interface between the filled (wet) part of the porous preform and the unfilled (dry) part. A justification of this assumption for certain process regimes can be found, e.g., in [39]. For the approach dealing with an unsaturated subregion we refer to the discussion in [9]. In the next section we recall the 3-D model from [18, 19, 20, 21, 39] which treats Newtonian fluids, but accounts for the deformation of the preform and for the curing. The third section is devoted to a more detailed discussion of the model for the 1-D case. The fourth section concerns an extension of this model to the case of the non-Newtonian fluids.

Parameter (i.e., permeability) identification is discussed in Section 3 in the Newtonian case and in Section 4 in the non-Newtonian case. In Section 5 the Forchheimer law is formulated instead of Darcy's law for large flow velocities, when inertial effects become important.

The evaluation of the permeability of a porous material is a very important step in optimization of liquid composite moulding technologies. Currently, the most reliable method for the determination of the permeability is experimental [35]. But it is well known that this approach inherits several major drawbacks (see, [3]). Therefore, a lot of efforts are focused on alternative ways for the evaluation of permeability. The investigations are done on *micro-* and *macro*–scales. For simple preform structures, i.e. unidirectional fiber arrays, random mats, or simplistic fabric–like structures, the results of permeability modeling on the micro–scale are presented in [12, 22, 37, 41]. Simulation on macroscale leads to solving systems of PDE describing the flow of liquid in the porous media, and here some general assumptions on the dependence of the flow velocity on the permeability are usually done a-priori. We should mention that in all experiments the macro–scale behaviour of the flow is observed, thus the interpretation and comparison of the results obtained using a numerical approach are much simpler for macro-scale models. We also mention a paper of Ghaddar [15], where a parallel computational approach for the evaluation of the permeability of unidirectional fibrous media is presented.

The determination of the permeability is critical for the simulation of the filling. Once the permeability is known, the polymer injection can be simulated by analytical or numerical methods. Analytical solutions for the infiltration front position are presented in Section 6 for both cases: Newtonian and non-Newtonian fluids. This information is related to the task of evaluation of permeability and determination of fluid properties.

Section 7 is devoted to a numerical algorithm for solving the governing system of PDEs. Finite volume discretization, treating the moving boundaries, decoupling of the system and results from some numerical experiments, are consecutively discussed there. An algorithm in Lagrangian coordinate system is presented in Section 8. In the last section the results of numerical simulations are presented and discussed.

Some preliminary results of this report were published in [10].

2 Mathematical Model

In this section we introduce the basic equations describing the injection moulding processes. Consider a *deformable* porous medium that at time $t = 0$ starts being infiltrated. Let us denote by D^w and D^d the time-varying domains corresponding to the wet part of the solid preform (i.e., which is already wet by the infiltrating resin), and to the dry one (i.e., which is not yet reached by the liquid polymer), respectively.

We assume that *capillary phenomena* can be neglected, thus D^w and D^d are divided by a sharp interface σ^i that represents the infiltration front. We also neglect the *gravity* force. Both assumptions are reasonable when the applied external pressure is relatively high. Let us denote by σ^e the contact surface between the pure liquid and the wet solid.

The mathematical model consists of evolution equations for the *state variables* in the wet and in the dry regions, completed by interfaces conditions on σ^i and σ^e and by proper boundary conditions. Note that the general multi-component mixture equations can be simplified [20] for the considered case.

2.1 Mathematical Model in the Wet Region

The following variables are used to describe processes in the wet region:

Φ_s^w and Φ_l^w are the volume fraction occupied by the solid and the liquid constituents, respectively. Assuming full saturation, the volume fraction occupied by the liquid satisfies

$$\Phi_l^w = 1 - \Phi_s^w \, .$$

$\mathbf{v}_s^w, \mathbf{v}_l^w$ denote the velocities of the solid and the liquid constituents. P_l^w is the pore liquid pressure. θ^w is the temperature of the mixture in the wet region. Here we assume that the solid and liquid constituents there are locally in thermal equilibrium. δ is the degree of cure of the resin.

Additionally, the model takes into account the fact that during the penetration the liquid undergoes a polymerization process (i.e., *curing*), which is largely exothermic. The degree of cure δ represents the fraction of cured resin. So $0 \leq \delta \leq 1$ (no curing for $\delta = 0$, complete curing for $\delta = 1$).

2.1.1 Mass Conservation of Solid and Liquid Constituents

Assuming that the solid and liquid are incompressible (i.e., the densities of the solid ρ_s and liquid ρ_l are constant), we obtain the local mass conservation equations in the Eulerian framework:

$$\frac{\partial \Phi_s^w}{\partial t} + \nabla \cdot (\Phi_s^w \mathbf{v}_s^w) = 0\,, \tag{1}$$

$$\frac{\partial \Phi_l^w}{\partial t} + \nabla \cdot (\Phi_l^w \mathbf{v}_l^w) = 0\,. \tag{2}$$

Assuming saturation the volume fraction occupied by the liquid is given by

$$\Phi_l^w = 1 - \Phi_s^w\,. \tag{3}$$

Summing up Eqs. (1) and (2) and introducing the *composite velocity* (or *volume average* velocity)

$$\mathbf{v}_c^w = \Phi_s^w \mathbf{v}_s^w + \Phi_l^w \mathbf{v}_l^w\,,$$

and recalling the saturation condition (3) results in the equation

$$\nabla \cdot \mathbf{v}_c^w = 0\,. \tag{4}$$

Let us denote by ρ_m^w the density of the mixture as a whole, i.e.:

$$\rho_m^w = \rho_s \Phi_s^w + \rho_l \Phi_l^w$$

and by $\mathbf{v}_m^w$ the *mass average* velocity of the mixture

$$\mathbf{v}_m^w = \frac{\rho_s \Phi_s^w \mathbf{v}_s^w + \rho_l \Phi_l^w \mathbf{v}_l^w}{\rho_m^w}\,.$$

Summing up Eqs. (1) and (2) multiplied by the corresponding densities gives the following mass conservation equation

$$\frac{\partial \rho_m^w}{\partial t} + \nabla \cdot (\rho_m^w \mathbf{v}_m^w) = 0\,.$$

2.1.2 Momentum Balance Equations

We will not consider the general momentum balance equations. To focus on flow in porous media, the following simplifying assumptions are used [20]:

(A1) Negligible surface tension and capillary effects and slow liquid flow in the porous medium;

(A2) Negligible liquid excess-stress; excess interaction force between the solid and the liquid is proportional to the velocity difference $\mathbf{v}_l^w - \mathbf{v}_s^w$;

(A3) Negligible inertia if compared to the stresses; external body forces (e.g. gravity) are neglected;

Then we write the general momentum balance equations as

$$\Phi_l^w(\mathbf{v}_l^w - \mathbf{v}_s^w) = -\frac{\mathbf{K}}{\mu}\nabla P_l^w\,, \tag{5}$$

$$\nabla P_l^w - \nabla\cdot\mathbf{T}_m^w = 0\,, \tag{6}$$

where μ is the liquid viscosity, which depends on the degree of cure δ and on the temperature θ^w, i.e.

$$\mu = \mu(\theta^w, \delta)\,.$$

The viscosity decreases with increasing temperature and increases with increasing degree of cure. Models used for the description of the viscosity are the following:

$$\mu(\theta,\delta) = \bar{\mu}\exp\left(\frac{A}{\theta}\right)\left(\frac{\delta_g}{\delta_g-\delta}\right)^{c+d\delta}, \quad \mu(\theta,\delta) = \bar{\mu}\exp\left(\frac{A}{\theta}+c\delta\right).$$

$\mathbf{K}$ is the *permeability* tensor, which for saturated deformable porous media depends on the deformation gradient $\mathbf{F}_s$ of the solid constituent $\mathbf{K} = \mathbf{K}(\mathbf{F}_s)$. P_l^w is the pore liquid pressure and $\mathbf{T}_m^w$ is the effective stress tensor.

Equation (5) is known as *Darcy's law* for deformable porous media. Here the effects of gravity are neglected, since normally for resin injection processes the pressure gradient is large compared to the value of the gravitation term. A critical discussion of the hypotheses underlying Darcy's law is given in [32, 34]. Several generalizations of Darcy's law can be used here, e.g. Forchheimer law to account for fast flows, or correction to take into account the non-Newtonian properties of the resin. Both generalizations are discussed in the next sections.

To complete the model, one has to specify the constitutive equation for the stress tensor $\mathbf{T}_m^w$. We will present such equations later for the one–dimensional case of the model.

2.1.3 Energy Balance

Following the same procedure, which was used in previous sections, it is possible to write the energy equation for the mixture:

$$\rho_m c_m \left(\frac{\partial \theta^w}{\partial t} + \mathbf{v}_m^w \cdot \nabla \theta^w \right) = \nabla \cdot (\mathbf{\Lambda}_m^w \nabla \theta^w) + \frac{1}{\mu} \mathbf{K} \nabla P^w \cdot \nabla P^w \tag{7}$$
$$+ \Phi_l^w H_c f_c(\delta, \theta^w) - \frac{\rho_s \rho_l \Phi_s^w \Phi_l^w}{\rho_m} (c_l - c_s)(\mathbf{v}_l^w - \mathbf{v}_s^w) \cdot \nabla \theta^w \, ,$$

where c_m is the specific heat of the mixture:

$$c_m = \frac{\rho_s \Phi_s^w c_s + \rho_l \Phi_l^w c_l}{\rho_m} \, .$$

$\mathbf{\Lambda}_m^w$ is the thermal conductivity tensor of the entire mixture, the term $\Phi_l^w H_c f_c(\delta, \theta^w)$ represents the heat generated by the curing reaction of the resin and the last term represents the heat diffusion due to the relative motion.

2.1.4 The Degree of Curing

As the liquid is moving, the evolution of the degree of cure is modeled by the equation

$$\frac{\partial \delta}{\partial t} + \mathbf{v}_l^w \cdot \nabla \delta = f_c(\delta, \theta^w) \, , \tag{8}$$

where f_c is an experimentally determined function describing the chemical reaction. The most popular model is proposed by Kamal–Sorour:

$$f_c(\delta, \theta) = (K_1 + K_2 \delta^m)(1 - \delta)^n, \quad K_i = c_i exp \left(- \frac{E_i}{R\theta} \right) \, ,$$

where R is the universal gas constant, E_i are the activation energies and c_i are the characteristic constants for the reactions.

2.2 Mathematical Model in the Dry Region

We proceed in a way similar to the one outlined for the wet region. However, some additional assumptions are used, which enable us to simplify the model.

(D1) The air pressure is everywhere equal to the atmospheric pressure;

(D2) The gas contribution to the global stress may be neglected;

(D3) The mass average velocity is equal to the velocity of the solid constituent and the composite density $\rho_m \approx \Phi_s^d \rho_s$, but the composite velocity

$$\mathbf{v}_c = \Phi_s \mathbf{v}_s + (1 - \Phi_s)\mathbf{v}_{air}\,.$$

Thus, we have the following state variables in the dry region: Φ_s^d is the solid volume fraction, $\mathbf{v}_s^d$ is the solid velocity and θ^d is the temperature.

Mass Conservation The equation of mass conservation reads

$$\frac{\partial \Phi_s^d}{\partial t} + \nabla \cdot (\Phi_s^d \mathbf{v}_s^d) = 0\,. \tag{9}$$

Momentum Balance Equation The deformation of the dry solid part is governed by the momentum balance equation

$$\nabla \cdot \mathbf{T}_s^d = 0\,, \tag{10}$$

where $\mathbf{T}_s^d$ is the stress tensor of the dry medium. Here we assume, that $\mathbf{T}_m^d = \mathbf{T}_s^d$.

As mentioned above, in order to complete the model we still have to specify the constitutive equations for the stress tensors $\mathbf{T}_m^w$ and $\mathbf{T}_s^d$. We assume that the wet and dry solids behave *elastically.*

Energy Balance Equation The Energy balance equation reads

$$\rho_s \Phi_s^d c_s \left(\frac{\partial \theta^d}{\partial t} + \mathbf{v}_s^d \cdot \nabla \theta^d \right) = \nabla \cdot \left(\Phi_s^d \mathbf{\Lambda}_s^w \nabla \theta^d \right)\,, \tag{11}$$

where $\mathbf{\Lambda}_s^w$ is the thermal conductivity of the solid.

2.3 Interface and Boundary Conditions

Infiltration Front

Let the infiltration interface σ^i be given by the surface

$$\psi_i(x, y, z, t) = 0\,.$$

This surface moves together with the propagation of the liquid, thus its evolution equation is given by

$$\frac{\partial \psi_i}{\partial t} + \mathbf{v}_l^w(\sigma^i) \cdot \nabla \psi_i = 0\,. \tag{12}$$

Preform Border

Let the contact surface σ^e between the liquid and the wet solid be given by

$$\psi_e(x, y, z, t) = 0\,.$$

As the resin penetrates the porous solid this material surface is fixed on the solid, and therefore its evolution equation is

$$\frac{\partial \psi_e}{\partial t} + \mathbf{v}_s^w(\sigma^e) \cdot \nabla \psi_e = 0\,. \tag{13}$$

Jump Conditions for Material Surfaces

Considering the mixture as a whole, the following jump conditions are obtained for material surfaces [18, 20, 31]

$$[\rho_m(\mathbf{v}_m - \mathbf{v}_\sigma)] \cdot \mathbf{n}_\sigma = 0\,, \tag{14}$$
$$[\theta] = 0\,, \tag{15}$$
$$[-P_l\,\mathbf{I} + \mathbf{T}_m] \cdot \mathbf{n}_\sigma = 0\,, \tag{16}$$
$$[P_l] = 0\,, \tag{17}$$

where $\mathbf{n}_\sigma$ is the normal outside D^w. It follows from (14) that

$$[\mathbf{v}_c] \cdot \mathbf{n}_\sigma = 0\,.$$

Using (16), (17) gives the continuity of the stress $\mathbf{T}_m$ across the the surface:

$$[\mathbf{T}_m] \cdot \mathbf{n}_\sigma = 0\,.$$

In the one-dimensional case assuming the same constitutive equation of elastic type for wet and dry solids, this implies the continuity of Φ_s across σ^i, and then we get from (14) the continuity of $\mathbf{v}_s$.

If the specific heat of the solid is continuous across σ^i, the temperature fluxes satisfy the following condition:

$$[\mathbf{\Lambda}_m \nabla \theta] \cdot \mathbf{n}_\sigma = 0\,.$$

Boundary Conditions on σ^e

Let the superscript $^-$ denotes the quantities evaluated in the pure liquid region. Then we have the following conditions

$$\Phi_s^- = 0, \quad \mathbf{v}_l^- = \mathbf{v}_{in}\,,$$
$$\mathbf{T}_m^-\,\mathbf{n}_{\sigma^e} = 0, \quad P_l^- = P_0\,,$$

where $\mathbf{v}_{in}$ is the inflow velocity of the resin and P_0 the pressure driving the flow. Thus, in the wet region we have $\Phi_s^w(\sigma^e, t) = \Phi_r$, where Φ_r is the solid volume fraction in the dry undeformed preform.

The temperature on σ^e is $\theta = \theta_{in}$, where θ_{in} is the temperature of the infiltrating liquid.

Boundary Conditions for the Curing Equation

The curing equation (8) is hyperbolic. Hence, the boundary conditions

$$\delta(\sigma^e) = \delta_{in}$$

must be specified on the part of the boundary where the characteristics enter the domain (the resin enters the preform), i.e. where $(\mathbf{v}_l^w - \mathbf{v}_s^w) \cdot \mathbf{n}_{\sigma^e} < 0$.

3 One-Dimensional Infiltration

This section deals with one-dimensional problems (see [1, 18, 20, 21]). Unidirectional injection is obtained in a flat mold of constant thickness when one side of the mold is connected to an injection channel. It is assumed that the permeability is homogenous and boundary effects can be neglected. Then the flow front is a straight line and the 1D model can be used to describe this case.

Assume that the porous medium is initially dry, homogeneous, isotropic and that the flow and the strain take place only along the x axis. Let us denote by $x = x_e(t)$ the left border of the preform, which can move (due to the preform's compression) when the liquid touches it. The infiltration front $x = x_i(t)$ separates the wet region D^w from the remaining dry region D^d:

$$D^w = [x_e(t), x_i(t)], \quad D^d = [x_i(t), L] .$$

As infiltration proceeds, the dry and the wet preforms compress or expand back according to the process conditions.

The one-dimensional mathematical model is obtained from the system of equations given in the previous section.

For $t \leq 0$ the whole preform is dry, at rest, and compressed at a given volume ratio:

$$\begin{cases} \Phi_s^d(x, t = 0) = \Phi_r, \quad x \in [0, L] , \\ x_e(t = 0) = 0, \quad x_i(t = 0) = 0 , \end{cases}$$

where Φ_r is the solid volume fraction of the solid preform in its undeformed configuration.

3.1 Wet Region

In the wet region the following equations are satisfied:

$$\frac{\partial \Phi_s^w}{\partial t} + \frac{\partial}{\partial x}(\Phi_s^w v_s^w) = 0\,, \tag{18}$$

$$\Phi_s^w(x_e(t), t) = \Phi_r\,, \;\; t > 0\,,$$

$$\frac{\partial v_c^w}{\partial x} = 0\,, \tag{19}$$

$$(1-\Phi_s^w)(v_l^w - v_s^w) = -\frac{K}{\mu(\delta,\theta^w)}\,\frac{\partial P_l^w}{\partial x}\,, \tag{20}$$

$$\frac{\partial P_l^w}{\partial x} = \frac{\partial \tau^w}{\partial x}\,, \tag{21}$$

$$\rho_m c_m\left(\frac{\partial \theta^w}{\partial t} + v_m^w\frac{\partial \theta^w}{\partial x}\right) = \frac{\partial}{\partial x}\left(\lambda_m\frac{\partial \theta^w}{\partial x}\right) + \frac{\rho_s\rho_l}{\rho_m}(c_l - c_s)\Phi_s^w$$
$$\times\,\frac{K}{\mu(\delta,\theta^w)}\frac{\partial \tau^w}{\partial x}\frac{\partial \theta^w}{\partial x} + (1-\Phi_s^w)H_c f_c(\delta,\theta^w) + \frac{K}{\mu(\delta,\theta^w)}\left(\frac{\partial \tau^w}{\partial x}\right)^2\,, \tag{22}$$

$$\frac{\partial \delta}{\partial t} + v_l^w\frac{\partial \delta}{\partial x} = f_c(\delta,\theta^w)\,, \tag{23}$$

where τ^w is the xx component of $\mathbf{T}_m$:

$$\tau^w = (\mathbf{T}_m)_{xx}\,, \;\; x\in D^w,\; t\geq 0\,,$$

and K is the xx component of the permeability tensor $K = (\mathbf{K})_{xx}$.

3.1.1 Constitutive Models

We still need to specify the constitutive equations for the stresses. At equilibrium the stress is usually related to the strain by a nonlinear relation, which can be determined by static stress–strain measurements. It should be noted that in one–dimensional problems the strain is related to volume ratio, i.e. to Φ_s.

Two models can be used.

(WA1) The elastic model for the wet porous medium preform reads

$$\tau^w = -\Sigma_w(\Phi_s^w)\,,$$

where Σ_w is a strictly increasing function. Frequently, it is assumed that

$$\Sigma_d = \Sigma_w \,.$$

Then the continuity of the stress across x_i implies also the continuity of the Φ_s. If wet and dry preforms behave elastically with $\Sigma_d \neq \Sigma_w$, the continuity of Φ_s across x_i does not hold any more.

(WA2) Due to the fact that the solid and the liquid matrices can not deform independently but have to carry the load by joint deformations, the wet preform can be modeled using a nonlinear Kelvin–Voigt law:

$$\lambda \left(\frac{\partial \tau^w}{\partial t} + v_s^w \frac{\partial \tau^w}{\partial x} \right) + \tau^w = \Lambda \left(\frac{\partial \Sigma_w(\Phi_s^w)}{\partial t} + v_s^w \frac{\partial \Sigma_w(\Phi_s^w)}{\partial x} \right) + \Sigma_w(\Phi_s^w) \,,$$

where λ is called the relaxation time, Λ is the retardation time, and the following inequality $\Lambda \geq \lambda$ is satisfied. If $\lambda = \Lambda$ and suitable initial conditions are used, then this equation has the solution:

$$\tau^w = -\Sigma_w(\Phi_s^w) \,,$$

i.e. the material behaves elastically.

(DA3) The dry preform is always assumed to behave elastically

$$\tau^d = -\Sigma_d(\Phi_s^d) \,, \tag{24}$$

where Σ_d is a strictly increasing function of the solid volume fraction.

3.1.2 Velocity Driven Infiltration

Before formulating equations in the dry region D^d we will use equation (19), from which it follows that v_c is space independent in D^w

$$v_c(x,t) = v(t) \,.$$

The boundary $x_e(t)$ is fixed to the solid phase and moves with the velocity v_s. Specializing the jump condition formulated in the previous section and writing it for the one–dimensional problem

$$[\rho_m(v_m - v_s)] = 0 \,,$$

one can obtain the following equalities:

$$\rho_m(v_m - v_s) = \rho_l \Phi_l (v_l - v_s) = \rho_l (v_c - v_s) \,.$$

Taking the limits on both sides of the boundary we prove that the composite velocity is continuous across $x_e(t)$, and thus we have:

$$v_c(x,t) = u_{in}(t), \quad x \in D^w \,.$$

Here $u_{in}(t)$ is the velocity of the infiltrated liquid.

Using Darcy's law (20) we can express the velocities of the solid and liquid constituents

$$\begin{aligned} v_s^w &= u_{in} + \frac{K}{\mu}\frac{\partial P_l^w}{\partial x}\,, \\ v_l^w &= u_{in} - \frac{\Phi_s^w}{1-\Phi_s^w}\frac{K}{\mu}\frac{\partial P_l^w}{\partial x}\,. \end{aligned} \tag{25}$$

The infiltration front $x_i(t)$ moves with the liquid, thus we have the initial value problem

$$\begin{cases} \dfrac{dx_i(t)}{dt} = v_l^w(x_i(t),t) = u_{in} + \left(\dfrac{\Phi_s^w}{1-\Phi_s^w}Q\right)(x_i(t),t)\,, \\ x_i(t=0) = 0\,, \end{cases} \tag{26}$$

where Q is given by

$$Q = -\frac{K}{\mu}\frac{\partial P_l^w}{\partial x} = -\frac{K}{\mu}\frac{\partial \tau^w}{\partial x}$$

and evaluated at the infiltration front from the wet region.

Determination of the Permeability

It follows from (25) that the permeability of the homogeneous structure can be determined as

$$K = (u_{in} - v_l^w)\ \frac{(1-\Phi_s^w)\mu}{\Phi_s^w}\ \left(\frac{\partial P_l^w}{\partial x}\right)^{-1}\,,$$

if experimental measurements of the interface velocity $v_l^w(x_i(t),t)$, the volume fraction occupied by the solid Φ_s^w and pressure gradients are available.

3.2 Dry Region

Since the interaction between the air and the solid can be assumed negligible, there is no pressure drop in the air. Therefore $P^d(x,t) = P_{atm}$, where P_{atm} is the atmospheric pressure.

Let τ^d be the xx component of the excess stress tensor in the dry region, then we obtain

$$\frac{\partial \tau^d}{\partial x} = 0 \,. \tag{27}$$

If the dry preform is assumed to behave elastically, then equations (24) and (27) imply that Φ_s^d is space independent, i.e.

$$\Phi_s^d = \Phi_s^d(t) \,. \tag{28}$$

Then the continuity equation implies that

$$\frac{\partial \Phi_s^d}{\partial t} + \Phi_s^d(t)\frac{\partial v_s^d}{\partial x} = 0$$

and the velocity satisfies the linear ODE with respect to the space coordinate:

$$\frac{\partial v_s^d}{\partial x} = -\frac{\frac{d}{dt}(\Phi_s^d(t))}{\Phi_s^d(t)} \,. \tag{29}$$

Integrating equation (29) over the interval $[x_i, L]$ and using the boundary condition

$$v_s^d(L,t) = 0 \,,$$

(i.e. the preform is constrained by a fixed draining boundary at $x = L$ and its velocity vanishes there), one has

$$v_s^d(x,t) = \frac{\frac{d}{dt}(\Phi_s^d(t))}{\Phi_s^d}(L - x) \,.$$

Neglecting the influence of the air, we get the simplified heat equation

$$\rho_s c_s \left(\Phi_s^d \frac{\partial \theta^d}{\partial t} + \frac{d\Phi_s^d}{dt}(L-x)\frac{\partial \theta^d}{\partial x} \right) = \frac{\partial}{\partial x}\left(\Phi_s^d \lambda_s \frac{\partial \theta^d}{\partial x} \right) \,. \tag{30}$$

3.2.1 Velocity Driven Infiltration

Now we will finish the analysis of this case. ¿From the general jump conditions formulated in the previous section (here we use the velocity of the infiltration interface) one can obtain the following equalities:

$$\rho_m(v_m - v_l) = \rho_s \Phi_s (v_s - v_l) = \rho_s (v_c - v_l) \,.$$

Then after simple computations it follows that v_c is also continuous across the interface $x_i(t)$

$$v_c^w(x_i(t),t) = v_c^d(x_i(t),t) \,,$$

thus it is equal to the inflow velocity

$$v_c(x,t) = u_{in}(t), \quad x \in D^d \,.$$

The continuity of v_c across the infiltration front and the fact that $x_i(t)$ is a material interface fixed on the liquid phase

$$\frac{dx_i(t)}{dt} = v_l(x_i(t), t)$$

leads to the initial value problem

$$\begin{cases} \dfrac{d}{dt}\Big(\big(1 - \Phi_s^d(t)\big)\big(L - x_i(t)\big)\Big) = -u_{in}(t)\,, \\ \Phi_s^d(0) = \Phi_{s0}^d\,. \end{cases} \tag{31}$$

The solution of (31) can be obtained in the explicit form:

$$\Phi_s^d(t) = \frac{1}{L - x_i(t)}\left(\int_0^t u_{in}(s)\,ds - x_i(t) + L\Phi_{s0}^d\right)\,. \tag{32}$$

This equation should be solved with the initial value problem (26), which specifies the development of the infiltration front $x_i(t)$.

3.2.2 Pressure Driven Infiltration

If the inlet pressure $\Delta P(t) = P_0(t) - P_{atm}$ is given, then we can integrate the momentum equation (21) and use the continuity of the stress on the infiltration front:

$$\tau^d(t) = \Delta P(t), \;\; t > 0\,.$$

Then the solid volume fraction of the dry region is given as

$$\Phi_s^d(t) = \Sigma_d^{-1}\big(\Delta P(t)\big)\,.$$

Using this formula and the mass conservation we can find the initial position of the left border of the preform after incoming liquid compresses the preform:

$$x_e(0) = L\left(1 - \frac{\Phi_r}{\Phi_s^d(0)}\right)\,.$$

Taking the equation (31) and using (25) to eliminate u_{in} from the obtained equation gives the initial value problem for the interface $x_i(t)$:

$$
\begin{cases}
\dfrac{d(\Phi_s^d x_i)}{dt} = L\dfrac{d\Phi_s^d}{dt} + \left(\dfrac{\Phi_s^w Q}{1-\Phi_s^w}\right)(x_i(t),t)\,, \\
x_i(0) = x_{i0}\,.
\end{cases}
\tag{33}
$$

The inflow velocity is then determined as

$$
\begin{aligned}
u_{in}(t) &= \Phi_s^d v_s + (1-\Phi_s^d) v_l \\
&= \big(L - x_i(t)\big)\frac{d\Phi_s^d(t)}{dt} + \big(1-\Phi_s^d\big)\frac{dx_i(t)}{dt}\,.
\end{aligned}
\tag{34}
$$

If $\Delta P(t)$ is constant in time, one obtains:

$$
u_{in}(t) = (1-\Phi_s^d)\,\frac{dx_i(t)}{dt}\,.
$$

4 Non-Newtonian Flow

In the previous section we considered Newtonian fluids, for which Darcy's law specifies the relation between the velocity and the pressure. But a large number of fluids, such as polymer solutions, polymer melts, suspensions do not follow Newton's law of viscosity [16]. The flow of polymer resin through fibrous materials is a very important process in the resin transfer moulding technology. The literature on non–Newtonian fluid flows is far less complete (see an overview in [45]). Some experimental results are presented in [44], a numerical study is given in [48].

One of the possibilities to describe non-Newtonian fluids is to modify the classical Darcy's law and to use a generalized Darcy's law (*power law*). For the one-dimensional case we have:

$$
(1-\Phi_s^w)(v_l^w - v_s^w) = \left(-\frac{K}{H}\,\frac{\partial P_l^w}{\partial x}\right)^{1/n}\,,
\tag{35}
$$

where n is used to describe different types of fluids. If $n < 1$ then a fluid is *pseudoplastic* (polymer solutions are pseudoplastic). *Dilatant* fluids are described using $n > 1$. Here H is the non-Newtonian bed factor. Following [8] we combine a power law model of a non-Newtonian fluid with the Blake-Kozeny model for the porous medium. We obtain

$$
H = \frac{\mu}{12}\left(9 + \frac{3}{n}\right)^n (150K\epsilon)^{(1-n)/2}\,,
$$

where ϵ is the porosity of the structure. Then equation (35) can be rewritten as:

$$(1-\Phi_s^w)(v_l^w - v_s^w) = \left(-\frac{K^{(1+n)/2}}{\mu\ d_n} \frac{\partial P_l^w}{\partial x} \right)^{1/n}, \tag{36}$$

$$d_n = \frac{1}{12}\left(9+\frac{3}{n}\right)^n (150\epsilon)^{(1-n)/2}.$$

Determination of the Permeability

Using the generalized Darcy's law (36) and the fact that v_c is constant in space we can express the velocity of the liquid constituent

$$v_l^w = u_{in} + \frac{\Phi_s^w}{1-\Phi_s^w}\left(-\frac{K^{(1+n)/2}}{\mu\ d_n} \frac{\partial P_l^w}{\partial x} \right)^{1/n}. \tag{37}$$

The infiltration front $x_i(t)$ moves with the liquid, thus we have the initial value problem

$$\begin{cases} \dfrac{dx_i(t)}{dt} = v_l^w(x_i(t),t) = u_{in} + \dfrac{\Phi_s^w}{1-\Phi_s^w}\left(-\dfrac{K^{(1+n)/2}}{\mu\ d_n} \dfrac{\partial P_l^w}{\partial x} \right)^{1/n}, \\ x_i(t=0) = 0\,. \end{cases}$$

After measuring the front velocity $v_l^w(x_i(t),t)$, the volume fraction corresponding to the solid Φ_s^w and the pressure gradient we can determine the permeability of the homogeneous structure as

$$K = \left(-\left((v_l^w - u_{in})\ \frac{1-\Phi_s^w}{\Phi_s^w} \right)^n \mu\, d_n \left(\frac{\partial P_l^w}{\partial x} \right)^{-1} \right)^{2/(1+n)}.$$

5 The Forchheimer law

Darcy's law states the linearity between velocity and pressure. It holds for slow flows when the inertial effects of the flow are negligible. In this section we consider one more correction to Darcy's law for large enough flow speed. Then the relation between the velocity and the pressure is nonlinear. The following equation has been proposed by Forchheimer and investigated by many authors (see, e.g. [2, 26, 29, 40]). We consider only the *one–dimensional* case of the equation

$$\frac{\mu}{K}u + \frac{\rho_l c_F}{K^{1/2}}\,|u|\,u = -\frac{\partial P_l^w}{\partial x}\,, \tag{38}$$

where $u = \Phi_l^w(v_l^w - v_s^w)$ and c_F is the Forchheimer or inertia coefficient. Eq. (38) is the two phase flow Forchheimer law for the case of moving porous medium (solid matrix), which means the relative velocity u must be taken instead of the usual $\Phi_l v_l$.

The nonlinear law (38) can be formulated as a Darcy-like law by introducing a velocity–dependent permeability $\hat{K}$ [29]:

$$\hat{K} = \frac{K}{1 + (K^{1/2}\rho_l c_F/\mu)|u|}\,. \tag{39}$$

So (38) is now written in the following form

$$\Phi_l^w(v_l^w - v_s^w) = -\frac{\hat{K}}{\mu}\frac{\partial P_l^w}{\partial x}\,.$$

6 One–Phase Model

It is well known that the macroscopic flow behavior at large length scales is well captured by one-phase flow models (see publications on RTM [9, 36, 47]). Such models are sufficiently accurate in predicting flow–front location, mold-filling time and pressure distribution during mold filling.

In this section we consider a one-dimensional model of the injection in a *non-deformable* porous medium (i.e., a rigid preform) with resin as a single phase.

Darcy's Law

Let us assume that the flow is governed by Darcy's law:

$$v = -\frac{K}{\mu}\frac{\partial P_l(x,t)}{\partial x}\,, \tag{40}$$

where $v = \Phi_l v_l$ is the volumetric velocity (i.e., the amount of volume traversing a unit area per unit time through the preform). We also assume that injection is *isothermal*

If the flow is saturated, then the assumption of resin incompressibility (i.e., the mass balance) leads to the following boundary value problem:

$$\begin{cases} \dfrac{\partial v}{\partial x} = 0\,, \\ P_l(0,t) = P_0(t), \quad P_l(x_i(t),t) = P_{atm}\,. \end{cases}$$

We obtain the solution in the explicit form

$$P_l(x,t) = P_0(t) + \frac{P_{atm} - P_0(t)}{x_i(t)}\, x\,. \tag{41}$$

The evolution of the infiltration front is described by the initial value problem

$$\begin{cases} \dfrac{dx_i(t)}{dt} = \dfrac{K}{\mu}\dfrac{P_0(t) - P_{atm}}{x_i(t)}\,, \\ x_i(0) = 0\,, \end{cases}$$

which integrates as

$$x_i^2(t) = \frac{2K}{\mu}\int_0^t (P_0(t) - P_{atm})\, dt\,.$$

If the driving pressure is constant in time (constant pressure driven infiltration) then we obtain the position of the infiltration front as:

$$x_i(t) = \sqrt{\frac{2K}{\mu}\,(P_0 - P_{atm})\ t}\,.$$

Determination of the Permeability

The established relationships can be used to evaluate the permeability K, if the positions of the flow front are recorded during the injection experiments and if the fluid viscosity μ is known:

$$K = \frac{\mu\, x_i^2(t)}{2\int_0^t (P_0(t) - P_{atm})\, dt}$$

or

$$K = \frac{\mu\, x_i^2(t)}{2(P_0 - P_{atm})t}\,. \tag{42}$$

We note, that one more relation for the evaluation of the permeability K follows directly from the infiltration front equation

$$K = \frac{\mu\, x_i(t)\, v_l\big(x_i(t),t\big)}{P_0(t) - P_{atm}}\,.$$

On inverse problems for determination of permeabilities. The problem of identification of diffusion coefficient in parabolic or elliptic equations arises in numerous engineering, medical and scientific applications. We want to reconstruct a diffusion coefficient from some additional data on a solution [11, 25, 49]. This data can consist in values of the solution (or functionals of this solution) measured on the boundary or in some points of the time-space region.

Generally, such inverse problems have notorious theoretical and numerical difficulties: non-monotonicity and severe ill–posedness, i.e. the inverse solutions are very sensitive to changes in input data resulting from measurement. Hence, they may not be unique. A regularization method should be used if we want to obtain a stable solution of the inverse problem [13, 17]. We apply such a regularization for determination of the permeability coefficient K in the form of the Least–squares method (see also [7]).

Let the positions of infiltration front $x_i(t_j)$ be recorded at specific time moments t_j, $j = 1, 2, \ldots, J$ during experiment. The objective function is defined as the sum of weighted differences between the front position $\bar{x}_i(t_j)$ predicted from the computational model and its corresponding measured value:

$$S(K) = \sum_{j=1}^{J} c_j \big(x_i(t_j) - \bar{x}_i(t_j)\big)^2 .$$

Identification of the Permeability Coefficient

1. For a given value of K solve the direct problem, describing the liquid moulding process.
2. Compute the objective function $S(K)$ and test the optimality of this value.
3. If the optimal value is not obtained, update the permeability K and goto step 1.

Gradient–type methods or the nonlinear Simplex algorithm can be used to minimize the objective function.

Even if we have an explicit formula (42) for the estimation of the permeability K, the regularization algorithm must be used to overcome the ill-posedness of such estimations due to errors in experimental data. A stable value of K is obtained taking the mean-value of all estimations:

$$K = \frac{\mu}{2J(P_0 - P_{atm})} \sum_{j=1}^{J} \frac{x_i^2(t_j)}{t_j} .$$

Velocity Driven Infiltration

It is well known that the velocity of the infiltration front must not be too slow to ensure a good quality of the final product. If the velocity is too slow it may result in the creation of air bubbles or voids between the fibers.

We can determine the pressure which is sufficient to produce a constant flow rate of the injected resin. Let us consider the following problem

$$\begin{cases} \dfrac{\partial v}{\partial x} = 0 \, , \\ v(0,t) = v_0, \quad P_l(x_i(t),t) = P_{atm} \, . \end{cases}$$

Integration of this equation yields

$$v(x,t) = v_0, \;\; 0 \le x \le x_i(t) \, .$$

Using Darcy's equation and integrating it, we finally get the relation:

$$P_l(0,t) = P_{atm} + \frac{v_0 \mu}{K} \, t \, ,$$

i.e. the pressure at the injection line should increase linearly with time.

The Generalized Darcy's Law

In this paragraph we assume that the flow is governed by the generalized Darcy's law (or *power* law):

$$v = \left(- \frac{K^{(1+n)/2}}{\mu \, d_n} \frac{\partial P_l(x,t)}{\partial x} \right)^{1/n} . \tag{43}$$

The explicit formula (41) is also valid for this case, thus similarly we obtain that for the generalized Darcy's law the infiltration front is given by

$$x_i(t) = \left(\frac{K^{(1+n)/2}}{\mu \, d_n} (P_0 - P_{atm}) \right)^{1/(n+1)} \left(\frac{n+1}{n} \, t \right)^{n/(n+1)} .$$

If front positions $x_i(t)$ are recorded during infiltration experiments, then the permeability K can be evaluated as

$$K = \frac{x_i^2(t)\,(\mu\, d_n)^{2/(n+1)}}{(P_0 - P_{atm})^{2/(n+1)}\,(\frac{n+1}{n}t)^{2n/(n+1)}}\,.$$

The Forchheimer Law

In this paragraph we assume that the flow is governed by the Forchheimer law

$$\frac{\mu}{K}v + \frac{\rho_l\, c_F}{K^{1/2}}\,|v|\,v = -\frac{\partial P_l}{\partial x}\,.$$

First, we will rewrite the formula for the modified permeability $\hat{K}$, when the dependence on velocity is substituted by a pressure gradient dependence (see, also [29]). Taking the absolute values of both sides of the equation and solving for positive root $|v|$, results in

$$|v| = \frac{\mu}{2\rho_l\, c_F K^{1/2}}\left(-1 + \left(1 + 4\gamma K^{3/2}|P'|\right)^{1/2}\right)\,,$$

where we use the notation $P' = \frac{\partial P_l}{\partial x}$ and $\gamma = \frac{\rho_l c_F}{\mu^2}$. Substituting this expression into (39) leads to the relation:

$$v = -\frac{2K}{\mu(1 + (1 + 4\gamma K^{3/2}|P'|)^{1/2}}\frac{\partial P_l(x,t)}{\partial x}\,.$$

The mass balance for the incompressible fluid flow gives the following nonlinear boundary value problem:

$$\begin{cases} \dfrac{\partial}{\partial x}\left(\dfrac{2K}{\mu(1 + (1 + 4\gamma K^{3/2}|P'|)^{1/2}}\dfrac{\partial P_l(x,t)}{\partial x}\right) = 0\,, \\ P_l(0,t) = P_0(t), \;\; P_l(x_i(t),t) = P_{atm}\,. \end{cases} \tag{44}$$

We see that the diffusion is selectively slowed down in places where the gradient of the solution is large. Such nonlinear diffusion problems are used for mathematical modeling of many important processes, e.g. for a nonlinear image processing [28, 33]. The existence and uniqueness of similar initial–boundary value problems is investigated in [6].

In general, solving nonlinear diffusion problem is a very difficult task, but assuming that the flow is saturated (thus K and μ are constant) we again obtain the solution in the following form:

$$P_l(x,t) = P_0(t) + \frac{P_{atm} - P_0(t)}{x_i(t)}\,x\,.$$

The evolution of the infiltration front $x_i(t)$ is described by the initial value problem

$$\begin{cases} \dfrac{dx_i(t)}{dt} = \dfrac{2K/\mu}{1+(1+4\gamma K^{3/2}|\frac{P_0(t)-P_{atm}}{x_i(t)}|)^{1/2}} \dfrac{P_0(t)-P_{atm}}{x_i(t)}\,, \\ x_i(0)=0\,. \end{cases}$$

Let us consider the constant pressure driven infiltration. Scaling the position of the infiltration front and the time with characteristic constants

$$x_i = 4\gamma K^{3/2}(P_0 - P_{atm})\,X, \quad t = 8\gamma^2 K^2 (P_0 - P_{atm})\mu\, t'$$

the initial value problem for the infiltration front can be rewritten as:

$$\begin{cases} \dfrac{dX^2(t')}{d\,t'} = \dfrac{2}{1+\left(1+\dfrac{1}{X(t')}\right)^{1/2}}\,, \\ X(0)=0\,. \end{cases}$$

In Figure 1 we plot the computed values of the infiltration front position $X^2(t')$. For the comparison we present also the position of the front obtained by using the Darcy law.

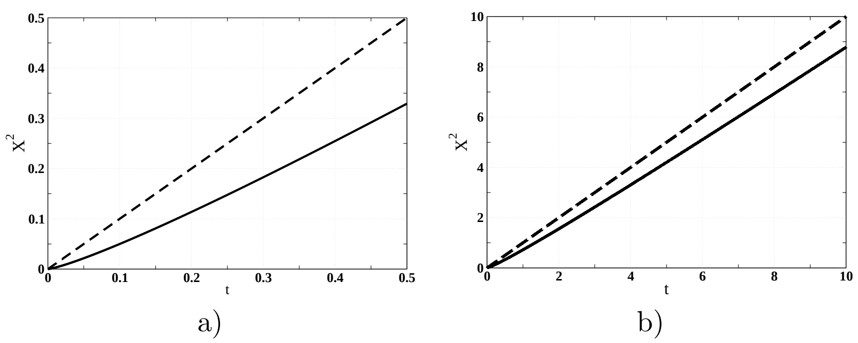

Figure 1: Position of $X^2(t)$: a) T = 0.5, b) T= 10. The solid line is a solution of the Forchheimer law, the dashed line is a solution of Darcy's law.

We have investigated the case of the pressure driven infiltration, when the pressure drop is constant. At the beginning the inertial effects are important and the velocity of infiltration front movement is slower for the Forchheimer law. But as the front moves forward the velocity decreases and the inertial effects become negligible. In this situation the flow again is described by the Darcy law.

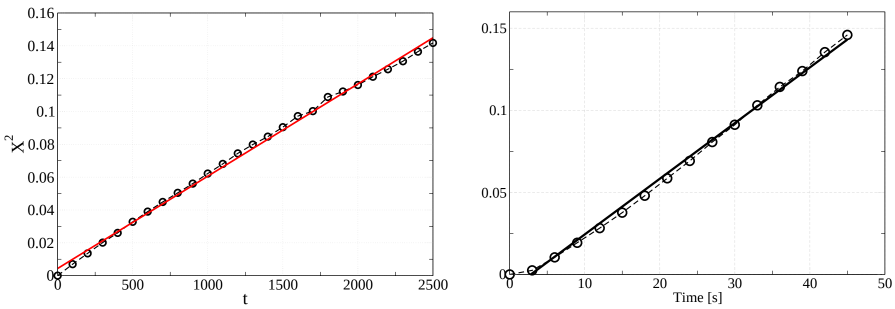

a) b)

Figure 2: Position of $x_i^2(t)$: measured values (circles) and a fitted curve (solid line).

Experimental Data

In this paragraph we present certain results of experimental measurements performed at the Institut fuer Verbundwerkstoffe GmbH, Kaiserslautern. The conditions of the experiment were characterized by a slow flow. A Newtonian liquid was used in experiments. In Figure 2 we plot the measured values of $x_i^2(t)$ (circles) and the linear approximation (solid line), which is fitted to the experimental data using the *Least squares* method. Experiments were done in conditions of pressure driven infiltration and two different values of pressure were used.

The results show that the model based on Darcy's law gives a good approximation of the movement of the infiltration front in this case.

Next we present measurements obtained with non-Newtonian liquids and compare them with our analytical predictions. Three different liquids were used in experiments. In Figure 3 we plot the measured values of $x_i^2(t)$. It can be seen that in two cases the liquids are close to Newtonian liquids and the last one shows a strong non-Newtonian behaviour.

We also estimated the parameter n in the generalized Darcy's law (35).

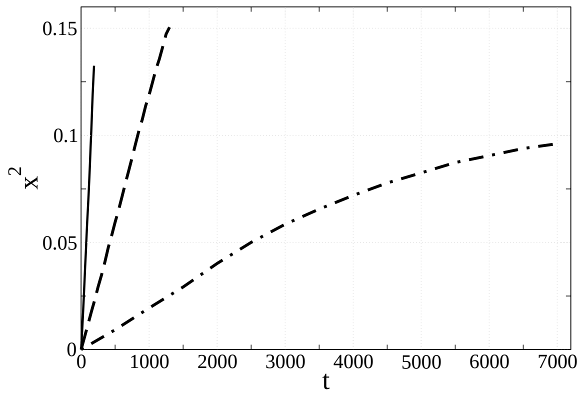

Figure 3: Position of $x_i^2(t)$ for non-Newtonian liquids.

The following technique was used: find n such that

$$M(n) = \min_{n \in [n_s, n_f]} \sum_{k=1}^{M} \big(x_i(t_k) - X_i(t_k, n) \big)^2 ,$$

where $x_i(t_k)$ are measured values of the front position, $X_i(t_k, n)$ are predicted values of the front

$$X_i(t_k, n) = \big(\, a(n) \, t_k + b(n) \, \big)^{\frac{n}{n+1}} ,$$

and $a(n), b(n)$ are obtained by using a linear fitting by the *Least squares* method of the transformed experimental data

$$\big(\, t_k, x_i(t_k)^{\frac{n+1}{n}} \, \big), \quad k = 1, \ldots, M \, .$$

The obtained results are presented in Table 1.

Table 1: The parameter n for non-Newtonian liquids

Liquid	n
$14 - 1$	1.16
$15 - 1$	0.975
$15 - 2$	0.40

It follows from the presented results, that the first and second fluid are very close to Newtonian liquids, but the third liquid can be described only by the generalized Darcy's law. In Figure 4 we plot the measured values $x_i(t_k)$ (for the third liquid) and predictions of the front position, given by the model based on the generalized Darcy's law with $n = 0.4$.

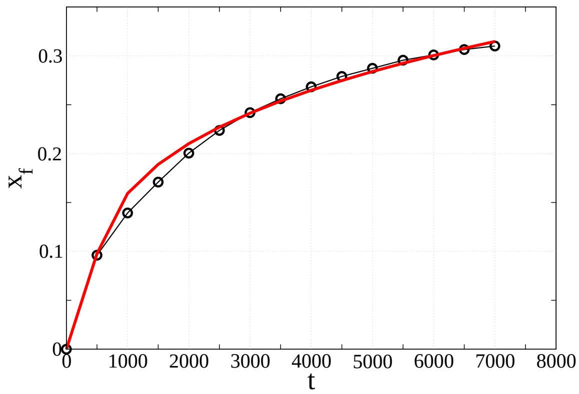

Figure 4: Measured and predicted positions of $x_i(t)$ for a non-Newtonian liquid.

7 Numerical Method

Let us assume that at time $t = 0$ the liquid touches the left border of the preform. We are not trying to describe the early instants of the infiltration process and simply state that the incoming liquid compresses the preform and wets some of its part, therefore the initial positions of the border x_e, as well as of the infiltration front x_i are given *a priori*

$$x_e(0) = x_{e0}, \quad x_i(0) = x_{i0} .$$

Then we can identify a wet region D^w and a dry region D^d.

There are two main difficulties in constructing discrete approximations of the given differential problem:

- Moving boundaries $x_e(t)$ and $x_i(t)$ (the Stefan type problem);
- The generalized Darcy's and Forchheinmer laws for flow velocities.